



Providing Choice & Value

Generic CT and MRI Contrast Agents



**FRESENIUS
KABI**

CONTACT REP

AJNR

**Beyond Diffusion Tensor MRI Methods for
Improved Characterization of the Brain after
Ischemic Stroke: A Review**

E.V.R. DiBella, A. Sharma, L. Richards, V. Prabhakaran, J.J.
Majersik and S.K. HashemizadehKolowri

This information is current as
of July 30, 2025.

AJNR Am J Neuroradiol 2022, 43 (5) 661-669

doi: <https://doi.org/10.3174/ajnr.A7414>

<http://www.ajnr.org/content/43/5/661>

Beyond Diffusion Tensor MRI Methods for Improved Characterization of the Brain after Ischemic Stroke: A Review

 E.V.R. DiBella,  A. Sharma,  L. Richards,  V. Prabhakaran,  J.J. Majersik, and  S.K. HashemizadehKolowri



ABSTRACT

SUMMARY: Ischemic stroke is a worldwide problem, with 15 million people experiencing a stroke annually. MR imaging is a valuable tool for understanding and assessing brain changes after stroke and predicting recovery. Of particular interest is the use of diffusion MR imaging in the nonacute stage 1–30 days poststroke. Thousands of articles have been published on the use of diffusion MR imaging in stroke, including several recent articles reviewing the use of DTI for stroke. The goal of this work was to survey and put into context the recent use of diffusion MR imaging methods beyond DTI, including diffusional kurtosis, generalized fractional anisotropy, spherical harmonics methods, and neurite orientation and dispersion models, in patients poststroke. Early studies report that these types of beyond-DTI methods outperform DTI metrics either in being more sensitive to poststroke changes or by better predicting outcome motor scores. More and larger studies are needed to confirm the improved prediction of stroke recovery with the beyond-DTI methods.

ABBREVIATIONS: AD = axial diffusivity; AK = axial kurtosis; DKI = diffusional kurtosis imaging; FA = fractional anisotropy; FM = Fugl-Meyer; GFA = generalized fractional anisotropy; MD = mean diffusivity; MK = mean kurtosis; NODDI = neurite orientation dispersion and density imaging; PLIC = posterior limb of the internal capsule; RD = radial diffusivity; SHORE = simple harmonic oscillator-based reconstruction and estimation; v_{ic} = neurite density; WMTI = white matter tract integrity

Stroke or a cerebrovascular accident is a problem worldwide, with 15 million people having a stroke annually, and it is a widespread cause of long-term disability and mortality.¹ MR imaging is a valuable tool for understanding and assessing brain changes after stroke and predicting recovery. Of particular interest is the use of diffusion MR imaging after the hyperacute stage, at 1–30 days poststroke. Thousands of articles have been published on the use of diffusion MR imaging in stroke, including several recent articles reviewing the use of DTI in stroke.^{2–4} The goal of this work was to survey and put into context the recent use of diffusion MR imaging methods beyond DTI, including diffusional kurtosis imaging (DKI),⁵ generalized fractional anisotropy (GFA),⁶ and neurite orientation dispersion and density imaging (NODDI) models,⁷ in patients poststroke. These methods use functional representations that either better match wider

ranges of diffusion data or tie to biophysical models that may better inform stroke studies. Early works report that these types of methods outperform DTI metrics.

Time Course of Ischemic Stroke


Approximately 87% of strokes are ischemic, while 13% are hemorrhagic; this review focuses on ischemic stroke. Because more ischemic strokes occur in the territory of the MCA than in other locations, most ischemic strokes affect the motor system. For example, 80% of individuals with stroke have impaired upper extremity motor function acutely.^{8,9}

The typical time course of ischemic stroke (Online Supplemental Data) begins with an acute phase in which ischemia results from development of either an in situ or embolic thrombus that lodges in a cerebral blood vessel, reducing or stopping blood flow to neural tissue served by that vessel. Soon after reduction of downstream blood flow, cytotoxic edema develops in the ischemic area and the cells in both gray and white matter swell, reducing the extracellular space from ~20% to 4%–10%.¹⁰ Such cell swelling is due to the lack of oxygen that impedes adenosine triphosphate production needed for active transport by Na^+/K^+ ATPase to keep Na ions in balance.¹⁰ Ischemic areas with blood flow of <10mL/100g become damaged in <6 minutes,¹⁰ creating an ischemic core.¹¹ Membrane configurations also change and form blebs,^{10,12} also termed

Received September 6, 2021; accepted after revision November 8.

From the Departments of Radiology and Imaging Sciences (E.V.R.D., A.S., S.K.H.), Occupational and Recreational Therapies (L.R.), and Neurology (J.J.M.), University of Utah, Salt Lake City, Utah; and Department of Radiology (V.P.), University of Wisconsin, Madison, Wisconsin.

Please address correspondence to Ed DiBella, PhD, UCAIR/Radiology and Imaging Sciences, 729 Arapahoe Dr, Salt Lake City, UT 84108; e-mail: Edward.dibella@hsc.utah.edu

 Indicates open access to non-subscribers at www.ajnr.org

 Indicates article with online supplemental data.

<http://dx.doi.org/10.3174/ajnr.A7414>

axonal beading.¹³ Acute treatments with tPA or catheter-based clot removal can be very helpful in limiting or avoiding neural damage if the patient presents early poststroke.

During the next weeks and months, the ischemic area turns into a necrotic core and the whole brain changes in a variety of ways. In the peri-ischemic area, Wallerian degeneration¹⁴ of the myelinated tracts is generally detectable at a few days poststroke and continues for months. Wallerian degeneration is the process of demyelination and disintegration of the distal axons that occurs after injury to a neuron. Axonal swelling is also characteristic of the early stage of Wallerian degeneration. Wallerian degeneration may occur both near and far from the ischemic bed. For example, rats with MCA occlusion exhibited Wallerian degeneration in the nonischemic corpus callosum.¹⁴

Lesions in one hemisphere also promote changes in the unlesioned (contralateral) hemisphere, depending on the amount of damage to the ipsilesional motor system. Degeneration of transcallosal fibers, increased branching and pruning of dendrites, and increased contralateral corticospinal tract sprouting have been reported.¹⁵ Jones and Adkins¹⁶ suggest that overcompensation with the nonparetic side promotes remodeling in the contralateral hemisphere and may cause synaptic competition with the lesioned hemisphere and reduce recovery in the paretic limb.

Neuroimaging with MR imaging plays several roles in stroke; the focus of this review is the use of diffusion MR imaging in the nonhyperacute-but-early stage 1–30 days poststroke, sometimes termed the subacute stage.

Diffusion MR imaging is widely used to assess and study stroke. MR imaging diffusion-weighted images reflect how water protons diffuse during short time spans. The water diffusivity depends on the local environment of the water protons. For example, in intact myelinated fibers, water protons diffuse with little restriction along the axon or fiber. In CSF, diffusion is isotropic and protons move relatively freely in all directions. While MR imaging diffusion images are acquired on millimeter scales, the diffusion reflects hindrances and restrictions to water mobility due to microstructures, with scales on the order of microns. Thus, diffusion provides information about the integrity of neural microstructures, but in a complicated way because the brain has a variety of neuronal cell bodies, axons, dendrites, and glial cells in each image voxel. The different compartments and the orientations of the fibers in the cell and the intra- and extracellular spaces influence the diffusion signal.¹⁷

Standard diffusion MR imaging acquires unweighted ($b = 0$) and diffusion-weighted images with diffusion weighting in multiple directions. Parameters such as ADC maps are calculated. The diffusion tensor signal representation uses a low-order cumulant expansion of diffusion¹⁸ and enables obtaining parameters such as fractional anisotropy (FA), mean diffusivity (MD), axial diffusivity (AD), and radial diffusivity (RD). Diffusion imaging and DTI have been reviewed in many places.¹⁹ The Online Supplemental Data show an example of some of these different parameters from DTI.

There has also been a tremendous amount of work, which is doubling every 2.9 years (see Fig 1 in Novikov et al²⁰), on diffusion MR imaging microstructural mapping techniques. These methods use higher-order signal expansions (such as DKI) or

other signal representations²¹ or model-based approximations to the biophysics. The motivation is that these models can be more specific to particular structures in a voxel and thus give more information regarding health or disease. The different signal representations and models are derived in different ways and require different data acquisitions than DTI, in particular with regard to q -space sampling and b -values (Online Supplemental Data). However, many of the parameters can be derived from the same acquisitions, and some of the studies listed in the Online Supplemental Data give parameters from several different representations or models, using the same data set. The Online Supplemental Data also show an example of some of these different parameters from most of the methods that are detailed later in this review.

For stroke, most of the work has focused on the corticospinal tract and white matter.²² Gray matter has been studied in healthy individuals with a NODDI model²³ and with a model designed for gray matter²⁴ (which may require very high b -values). There are limited studies using beyond-DTI microstructural mapping methods to look at gray matter in human subjects with stroke, though DKI⁵ and diffusion spectrum imaging²⁵ have been used.

Diffusion MR Imaging in Stroke

In regions of ischemic stroke, signal in diffusion-weighted images is decreased acutely.²⁶ The reason that diffusion decreases in stroke is not completely understood, though a number of studies give some insight into the process. For example, as described above, ischemic neurons undergo axonal swelling. If axons swell and intra-axon diffusion compared with extra-axonal diffusion is quite different, then having more intra-axonal space, which is more restricted to diffusion, could result in lower diffusion (and higher signal) on the MR images. However, a study using fluorodeoxyglucose molecules found that the molecule diffuses equally in both intra- and extracellular spaces and diffusion in both spaces decreases ($\sim 40\%$ ADC decrease) in ischemic conditions.²⁷ More recent works have evolved estimates of intra-axonal diffusion and its relation to extracellular diffusion.^{28–30} A likely partial explanation for slower, more restricted diffusion in stroke regions is that axons become “beaded,” more tortuous instead of purely cylindric structures so that the total cell surface area is preserved during the swelling.³¹ In this case, diffusion may become more restricted, especially in the axonal direction. Simulations have shown that water ADC decreases in beaded structures.^{13,31} Photomicrographs¹² and confocal microscopy have shown such structures.³²

Other factors such as the multiexponential diffusion change with b -value, water exchange, and the axonal g -ratio (outer-to-inner axon diameter ratio),²⁰ also play roles in imaging diffusion after stroke. Water exchange between fast and slow diffusion components has been studied,³³ and the biophysics of white matter in the context of diffusion imaging was reviewed by Nilsson et al.³⁴ More recently, a beyond-DTI method sensitive to exchange was proposed (Online Supplemental Data).³⁵

We move now to consider some of the works that illustrate how MR imaging has been used in the assessment of stroke and for prediction of stroke recovery.

Diffusion MR Imaging for Predicting Recovery from Stroke. Diffusion MR imaging has many potential uses in subacute stroke, including understanding the time course of brain changes, predicting the response to specific therapeutic interventions, and selecting and monitoring therapy. Predicting motor recovery has been a highly studied objective.²

Why Predict Recovery? Stroke research includes both hyperacute evaluation and treatment with thrombolysis or mechanical clot removal and less acute evaluation. “Time is brain,” and as described above, and for suitable patients presenting to the hospital within 24 hours, tPA and thrombectomy procedures often help recovery by reducing the extent of neural damage. Yet, while these procedures reduce damage from stroke, they usually do not eliminate such damage. After hyperacute procedures and for the ~80% of subjects who do not receive such intervention, rehabilitation is commonly needed. How the brain recovers after stroke and the best therapy and therapy timing for each stroke survivor after the hyperacute phase are open questions. Therapy within the first few weeks after stroke is likely to be more effective due to the heightened neuroplasticity potential at that time.

Predicting recovery is, thus, a highly sought-after goal.^{36–38} Accurate prediction is needed to plan discharge, set patient goals, choose therapy (therapies aimed at reducing impairment versus therapies to train compensation strategies and assistive technologies), and offer the patient a prognosis.³⁹ Recovery predictions also allow better testing of newly developed recovery therapies that hope to promote greater recovery than spontaneous recovery or current therapies.

Nonimaging Methods for Stroke Recovery Prediction. A variety of prediction methods have been used, such as those based on changes in the NIHSS,⁴⁰ but prediction methods that do not use imaging typically have poor specificity (36% in Hemmen et al⁴⁰) or only estimate a binary outcome (favorable or not favorable), which is not as useful clinically. Recovery depends, in part, on the size and the location of the ischemic area and on a variety of other factors such as demographics, systemic atherosclerosis, and social support networks.

Strokes causing motor deficits are commonly said to display proportional recovery—that is, in the first 3 months following stroke, 70% of the new impairment is recovered^{41–44} in most individuals, while the other individuals (“atypical responders”) have much less recovery. This finding is based on function at baseline measured with the Fugl-Meyer (FM) upper extremity assessment,⁴⁵ which has a range of 0–66. For example, $\Delta FM = 0.7 \times (66 - FM_{\text{initial}}) + 0.4$ predicted recovery reasonably well in 160 of 211 subjects.⁴³ However, it was recently shown by two separate groups that mathematic coupling and ceiling effects incorrectly biased the previous findings and that random recovery could give results similar to proportional recovery when the previously published analysis methods were used.^{46,47} Thus, we may understand recovery less than we think we do, and there is additional motivation for methods such as MR imaging to bolster our ability to characterize and predict recovery from stroke.

Imaging Methods for Prediction of Stroke Recovery. MR imaging methods such as diffusion, perfusion, fMRI, spectroscopy,

and T1- and T2-weighted images give insight into the location and severity of stroke.^{48,49} Perfusion imaging to delineate ischemic areas is typically used in concert with diffusion imaging at the hyperacute stage of stroke to see if the ischemic area exceeds (defining a larger area at risk) or matches the restricted diffusion area. Match/mismatch criteria can inform the hyperacute use of thrombectomy and tPA.⁵⁰ These methods are applied at the hyperacute stage and are typically less valuable for longer-term recovery prediction. fMRI was shown to relate more weakly to motor deficits than tract integrity based on diffusion imaging.⁵¹ Moreover, task fMRI relies on patient cooperation, effort, and ability to perform motor tasks, which may be compromised on the basis of the severity of stroke, though resting state functional connectivity may be promising.⁵² T1 and T2 methods are often used to size lesions but correlate relatively poorly with motor function compared with also considering lesion location and load on a fiber tract (gauged with diffusion imaging^{53,54}). Lesion load is also a relatively poor predictor of recovery. Adding DTI enables better assessment of stroke and prediction of recovery.

DTI Methods for Predicting Stroke Recovery

DTI uses a signal representation that is limited to representing, for example, a Gaussian distribution of diffusion displacement and a single fiber direction in each voxel, which may not accurately reflect the mixture of glia, myelin, neurons, extracellular space, CSF, and microvasculature that can exist within a voxel. Still, DTI metrics are sensitive to stroke-related changes, and numerous studies have used DTI to better understand and characterize changes after stroke^{48,54} and to gauge the effects of therapies.⁵⁵

While DTI and particularly FA are useful, histology studies have shown that FA is not a specific biomarker because it conflates myelination, fiber dispersion, and intra-/extraneurite contributions. FA is widely used despite its nonspecific nature. For example, a recent review⁴ reported good correlation between a DTI metric such as FA and a motor outcome metric such as FM or NIHSS (which is not as useful a measure of motor capabilities as FM) scores, though a few of the studies did not find significant predictive correlations from the FA metrics at some stages.^{56–58} Kumar et al² did a meta-analysis on 6 small studies with outcome measures such as NIHSS and reported a pooled $r = 0.82$. They pointed out the need for larger, prospective studies to better determine the utility of FA metrics for predicting outcomes. As highlighted below, these retrospective studies report best-fit linear correlations for the data obtained and would not be expected to perform as well when doing prospective predictions.

Tractography from DTI has also been useful for studying stroke and predicting recovery. For example, tractography methods for defining tract-based ROIs⁴ and connectivity analysis methods^{59,60} have been developed.

Diffusion methods stand to benefit from beyond-DTI methods that can in some ways consider crossing fibers, structural compartments with hindered or restricted diffusion, and non-Gaussian distributions of the diffusive motion of water in the brain. Here, we seek to complement the recent DTI in stroke reviews^{2–4} by focusing on works that used beyond-DTI methods for obtaining microstructural parameter maps in stroke. Several

studies have reported better correspondence of these microstructural mapping methods with motor outcomes, and others have reported greater changes between ipsilesional and contralesional regions in the microstructural parameters compared with DTI, implying greater sensitivity to stroke effects.

Beyond-DTI Methods for Stroke

New diffusion methods have been developed that better separate the diffusion signal contributions from fiber dispersion and intra-/extraneurite compartments. More samples in q -space (Online Supplemental Data) provide better angular resolution of fibers,⁶¹⁻⁶⁵ allow estimating the non-Gaussian portions of the signals (kurtosis), and enable estimating models of biophysical compartments along with fiber orientations and dispersions. Such compartment models are well-described in multiple articles, including the supplement in Lakhani et al.⁶⁶ Because the adverse impact of stroke is, in part, from disrupting white matter connectivity, better measures of assessing fiber bundle integrity could give better insight and predictive power over current techniques. This white matter assessment is one way that beyond-DTI methods may provide significant additional information. Currently, the only beyond-DTI methods used with stroke applications to date include the following: DKI, white matter tract integrity (WMTI), GFA, NODDI, simple harmonic oscillator-based reconstruction and estimation (SHORE) parameters, and 1 article using different diffusion times to estimate the rate of kurtosis.

DKI. The standard DTI representation is appropriate in freely diffusing isotropic media such as CSF. For areas with restricted diffusion such as within axons, Jensen et al⁶⁷ proposed extending the DTI signal representation to add a higher-order term:

$$\ln\left(\frac{S(b)}{S(0)}\right) = -bD + \frac{1}{6}b^2D^2K,$$

where K is the kurtosis. To have sufficient data to fit these higher-order terms uniquely, one must have data acquired at multiple nonzero b -values. As with DTI, a kurtosis tensor can be defined to take into account diffusion directions. When DKI is used to fit, the DTI tensor portion has 6 unknowns and the DKI tensor values include 15 unknowns, so at least 21 q -space samples and a $b=0$ image are typically needed. For typical brain microstructure and diffusion acquisition parameters, the non-Gaussian portion of the diffusion signal⁶⁸ will not be prevalent if $b \leq 1000 \text{ mm}^2/\text{s}$. Acquisitions vary but may include, for example, 15 directions at $b=1000$ and 15 directions at $b=2000$ (Online Supplemental Data). The additional microenvironment complexity in stroke may make DKI a better approach than DTI.

Most of the beyond-DTI research in stroke has been with DKI, with 10 articles in rat stroke models,⁶⁹⁻⁷⁸ a recent review article,⁷⁹ and 10 articles in humans (Online Supplemental Data). The rat model studies found larger changes with mean kurtosis (MK) and axial kurtosis (AK) compared with DTI metrics. Sizing of lesions was also studied with ex vivo MR imaging, and the studies found that DKI metrics such as MK were larger than those in MD and histology.^{72,78} However, with in vivo MR imaging and a different segmentation method, others reported that

the DKI metrics yielded lesion sizes smaller than MD volumes.⁷⁷ In addition, sizing has not been shown to be very predictive of motor recovery.⁸⁰ Possibly more promising from the rat model studies is that the DKI parameters changed more with time (or compared with the contralateral hemisphere) than the DTI parameters due to stroke. This increased sensitivity to stroke was also found in the studies with humans. The Online Supplemental Data summarize the details of each of these DKI human imaging poststroke articles.

The relatively widespread use of DKI compared with other beyond-DTI methods is likely due to modest acquisition requirements, GE Healthcare's early implementation of DKI in their FuncTool software on the scanner, and early reports of potential. For example, Hui et al,⁵ in 2012, reported that MK changed more than FA in stroke regions relative to the nonstroke hemisphere (ipsilesional and contralesional regions) in 44 subjects with stroke, though there was no evaluation of the clinical importance of such changes. Fast kurtosis methods using <20 diffusion-weighted images have also been developed⁸¹ and used in rat studies.^{71,74}

Ideally, FM scores at 6–12 weeks poststroke serve to measure motor outcomes, and such scores were measured in 2 DKI articles. In Spampinato et al,⁸² the MK ipsilesional/contralesional ratio gave the best correlation with FM scores ($r=0.85$). The AK ratio also was predictive ($r=0.78$), while DTI MD ($r=0.69$), and FA ($r=0.4$) ratios had lower associations with FM scores. Li et al⁸³ grouped patients into good responders (>10 -point FM change) or poor responders. Then a relative axial kurtosis AK measure (ipsilesional–contralesional)/contralesional gave the best discrimination of the 2 groups and was superior to DTI methods. The study in Yu et al⁸⁴ used NIHSS scores rather than FM and found lower correlations, but still the relative AK metric gave the highest correlation ($r=0.3$) with NIHSS scores. DTI methods in Yu et al showed no changes in the cortical spinal tract on the stroke side relative to the contralateral side (and hence no correlation with NIHSS).

The WMTI method was included in 2 of the DKI articles.^{5,82} WMTI assumes intra- and extra-axonal compartments and estimates axonal water fraction, intra-axonal AD, extra-axonal axial and radial diffusivities, and the tortuosity of the extra-axonal space. WMTI assumes all parallel axons and so is only applied in the corpus callosum, or where $FA > 0.3$.^{5,82} WMTI parameters were calculated along with DKI, and the axonal water fraction correlated ($r=0.63$) with FM scores in Spampinato et al.⁸² More recent nonstroke works relaxed the parallel axon requirement using a WMTI-Watson model that includes fiber dispersion, though the method assumes axially symmetric diffusion, so it was only applied in the spinal cord.⁸⁵

Besides DKI, other beyond-DTI methods have been explored for use in patients with stroke. The Online Supplemental Data summarize the 9 articles that have investigated other methods: GFA, SHORE, NODDI, and rate of kurtosis methods have all shown promising results in patients with stroke.

GFA. GFA is obtained from the orientation distribution function, which can be calculated from the 3D ensemble average propagator.²¹ The 3D ensemble average propagator is obtained, for

example, by 3D Fourier transform from Cartesian-sampled q -space data.⁸⁶ Then, similar to how FA is calculated from DTI data as $SD(\lambda) / RMS(\lambda)$, where λ is the eigenvalue of the diffusion tensor and RMS stands for root mean square, $GFA = SD(\varphi) / RMS(\varphi)$, where φ represents the orientation distribution function.²¹ GFA can be considered as an extension of FA in voxels that have crossing/touching fibers, so it may give a better measure of fiber disarray in stroke.

The GFA studies in the Online Supplemental Data came from diffusion spectrum imaging, which acquires a Cartesian grid of q -space samples with a relatively high b_{maximum} (4000–8000 s/mm²). Most of these studies took the unusual approach of studying only the contralesional side. GFA revealed microstructure changes in the contralesional side during poststroke remodeling.^{6,25,87–89} Most of these studies used the same data set of ~10 patients with stroke who had been imaged with a 26-minute diffusion acquisition.^{6,25,89} GFA in the contralesional side was highly predictive of the 6-month NIHSS score ($r^2 = 0.84$ adjusted).⁶ Combining GFA + NIHSS + age had an even higher correlation ($r^2 = 0.96$ adjusted) in this small study.⁶ Other parameters (SHORE) were also calculated from this data set, as described below.

SHORE. The SHORE method calculates propagator anisotropy, along with measures of the ensemble average propagator variance (mean square displacement), return-to-the-origin probability, the return-to-the-axis probability, and the return-to-the-plane probability.⁹⁰ These parameters when evaluated in a subcortical loop of tracts gave high correlations with 6-month NIHSS scores.⁹¹ Galazzo et al²⁵ added comparison with DTI and evaluated findings in gray matter. Both articles used the 10-person diffusion spectrum imaging data set from Granziera et al⁶ and evaluated only the contralesional side.

Compartment Model Methods. Unlike the FA, GFA, and SHORE parameters that arise from signal representations that do not postulate a particular underlying biophysical model, a number of compartment-based models have been developed. These models, of which NODDI is a good example, estimate microstructural multicompartiment (intra-axon, extra-axon, CSF compartments for NODDI) and fiber-dispersion parameters. This approach is thought to be useful for characterizing dispersed or crossing fibers⁹² and for estimating white matter degeneration in the subacute phase of stroke when Wallerian degeneration and glial scarring processes are occurring.⁹³ A few groups have recently reported NODDI models to be useful in stroke imaging in rats⁹⁴ and humans.^{7,95–97} These findings are despite the fact that NODDI fixes diffusivity parameters to 1.7 (and to 3.0 s/mm² in spinal fluid), and these parameters are not uniformly correct in healthy individuals and are less accurate in stroke regions. It is also known that NODDI “neurite density” (also called v_{ic}) does not reflect the density of neurites in tumor and in stroke (where it has been called the “restricted diffusion index”). The only NODDI study including outcome measures (FM scores) was Hodgson et al,⁹⁶ in which the best outcome predictor was found to be the orientation dispersion index (optimism-adjusted $r^2 = 0.83$), though v_{ic} (or the “restricted diffusion index”) also

correlated $r^2 = 0.70$, as did GFA ($r^2 = 0.57$). Other parameters including DTI and stroke size and lesion load did not correlate as well.

The two other NODDI stroke studies included DKI and also studied changes in microstructure across time.^{7,97} The study of Wang et al⁹⁷ was unpaired: The same subject was not imaged at multiple time points. Still, the percentage difference of the orientation dispersion index in the stroke area relative to the contralesional side was larger than other NODDI parameters, MK, FA, or MD. Correlation with time since stroke onset was also highest with the orientation dispersion index. Mastropietro et al⁷ analyzed only the posterior limb of the internal capsule (PLIC) and cerebral peduncle regions and reported significant differences between their ipsilateral and contralateral sides for the orientation dispersion index and other parameters including FA, AD, RD, kurtosis anisotropy, and AK. Other parameters (MD, MK, v_{ic} , isotropic volume fraction) did not show significant differences.

Other biophysical factors, such as different T2s in intra-axonal and extracellular compartments, water exchange, and Gaussian diffusion assumed in compartments, could all be of interest but are not included in the compartment model methods. Using different diffusion times while maintaining the same b -value is also of interest and was recently shown to help predict chronic stroke areas in 5 subjects with stroke.³⁵ That method estimated the exchange rate (rate of kurtosis) using an equation based on a 2-compartment model with exchange. Other models such as NODDI assume no water exchange between the myelin and the intracellular and extracellular compartments, though there is evidence for a mixture of fast and slow exchange.³⁴ Such exchange causes signal changes due to different diffusivities and relaxivities (possibly negligible) in the different compartments.⁹⁸ A multi-shell acquisition with 2 diffusion times was used in Lampinen et al³⁵ to obtain a parameter sensitive to the exchange rate. Results showed faster exchange in the ischemic stroke areas.³⁵

The Online Supplemental Data summarize the methods with outcome measures (FM or NIHSS) graphically, with the graph edges reflecting the number of subjects in each comparison.

Acquisition and Analysis Diversity in Beyond-DTI Methods

The beyond-DTI studies varied considerably in the acquisition. Besides a range of angular q -space sampling and different shells or b -values, there were wide differences in spatial resolution (0.94–3 mm in-plane, 1.5- to 4-mm section thickness), number of slices (range, 9–64), acquisition time (range, 2–27 minutes), and imaging time poststroke (range, 6 hours to 4 weeks). A large high-resolution highly sampled q -space data set similar to that with connectome imaging would be ideal to determine the value of higher resolution and sampling for the use of beyond-DTI methods in stroke.

Different acquisition parameters may lead to different results. This possibility is best known in DTI; for example, Table 1 in Barrio-Arranz et al⁹⁹ describes results from 14 studies of different spatial resolutions, b -values, or diffusion directions and how FA and MD changed. Less has been studied with beyond-DTI methods, but for example, NODDI results are a function of b -values and gradient directions.¹⁰⁰ This finding again is motivation for large rigorous studies in stroke with overcomplete sampling and outcome measures for validation.

Analysis methods tended to be from either ROIs in parts or all of the cortical spinal tract (PLIC, the cerebral peduncle, and the corona radiata) and/or from manually identified ischemic regions. Note that it has been shown in DTI that different fitting methods (linear, nonlinear) give significantly different results.¹⁰¹ Beyond-DTI methods such as a more rapid NODDI fitting method¹⁰² also are known to affect results compared with the original slower NODDI fitting method. A few studies used tract-based analyses and/or voxel-based analyses. Atlas-based regions were often used, though it is not known how well the atlas matches tracts in stroke regions with disrupted fiber tracts. Trade-offs with SNR and with how different beyond-DTI parameters vary with voxel size are yet to be studied in subjects with stroke. Even if ROI analysis methods are used, it could be that imaging with smaller voxels could better inform microstructure and tractography methods.

Note that for predicting stroke recovery and following stroke recovery, we are interested not only in local stroke effects but also global stroke effects. The best focus and most relevant information to understand and predict adaptations are still not known. For example, some have found the PLIC to be the most predictive of future motor function, even if the stroke was not in the PLIC. This finding may be because the PLIC is a hub with incoming sensory neurons and outgoing motor control neurons and the way that stroke, even in other regions, affects the PLIC is telling. Alternatively, this may simply be from the small sample size and limited comparisons with other fiber tracts; other regions or composites of regions may provide improved predictive information.

The different acquisitions, nonstandard processing, and few studies with relatively few subjects that include motor stroke outcomes mean that larger studies with FM scores and current acquisition techniques including simultaneous multislice methods¹⁰³ are needed to better understand the impact of beyond-DTI methods. While the scan times vary widely, from 2 to 27 minutes (Online Supplemental Data), this variation is, in part, due to limited coverage, spatial resolution, and *q*-space sampling choices. Acquisition requirements for optimal performance for the different methods are not yet known in stroke. It is likely that all of the beyond-DTI methods can be made clinically practical (<5 minutes) with advanced acquisition (simultaneous multislice) and deep learning techniques,¹⁰⁴ though those techniques are still evolving and being evaluated. Direct comparisons between the beyond-DTI methods and investigation into combining parameters from different methods should also be performed in the context of stroke.

Other Considerations

As pointed out by Kim et al,³⁸ 90% of neurologic biomarker studies, including most DTI studies as well as most nonimaging methods, did not use an independent set of stroke data to cross-validate their prediction model. Thus, the results are a best case of predicted correlation, retrospectively, with the given data set. The beyond-DTI studies reported in the tables here did not perform cross-validation, though 1 small study used *k*-fold cross-validation⁹⁶ to have more confidence in the predictive value. The studies also did not identify or discuss minimally clinically important differences,³⁸ which will be essential to further develop and translate these promising new methods to clinical use.

Another open question is how outcome predictions vary as a function of therapy. This question includes acute treatments such as tPA or thrombectomy and therapies such as brain-computer interface methods. The brain-computer interface has shown promising results in small studies of people with chronic stroke; recovery may be enhanced, especially if such therapies are started early after stroke. Indeed, advanced diffusion-based metrics may be able to predict who would benefit the most from the brain-computer interface or other types of therapies; plasticity or reorganization changes may be measurable with beyond-DTI parameters while confounding the interpretation of FA. The ability of diffusion methods to differentiate ipsilateral-versus-contralateral contributions of motor tracts to upper extremity function may also inform stroke rehabilitation approaches.¹⁰⁵

The many exciting new advances in neuroimaging and particularly in beyond-DTI methods are likely to have a highly significant impact in the context of predicting stroke recovery, for improving our understanding of brain changes after stroke, and for providing unique advantages when selecting personalized stroke therapy. However, this review also makes clear that there is a need for rigorous studies to better evaluate and translate these microstructural mapping methods to clinical application.

Disclosure forms provided by the authors are available with the full text and PDF of this article at www.ajnr.org.

REFERENCES

1. Roger VL, Go AS, Lloyd-Jones DM, et al; American Heart Association Statistics Committee and Stroke Statistics Subcommittee. **Heart disease and stroke statistics—2011 update: a report from the American Heart Association.** *Circulation* 2011;123:e18–e209 [CrossRef Medline](#)
2. Kumar P, Kathuria P, Nair P, et al. **Prediction of upper limb motor recovery after subacute ischemic stroke using diffusion tensor imaging: a systematic review and meta-analysis.** *J Stroke* 2016;18:50–59 [CrossRef Medline](#)
3. Puig J, Blasco G, Schlaug G, et al. **Diffusion tensor imaging as a prognostic biomarker for motor recovery and rehabilitation after stroke.** *Neuroradiology* 2017;59:343–51 [CrossRef Medline](#)
4. Moura LM, Luccas R, de Paiva JP, et al. **Diffusion tensor imaging biomarkers to predict motor outcomes in stroke: a narrative review.** *Front Neurol* 2019;10:445 [Medline](#)
5. Hui ES, Fieremans E, Jensen JH, et al. **Stroke assessment with diffusional kurtosis imaging.** *Stroke* 2012;43:2968–73 [CrossRef Medline](#)
6. Granziera C, Daducci A, Meskaldji DE, et al. **A new early and automated MRI-based predictor of motor improvement after stroke.** *Neurology* 2012;79:39–46 [CrossRef Medline](#)
7. Mastropietro A, Rizzo G, Fontana L, et al. **Microstructural characterization of corticospinal tract in subacute and chronic stroke patients with distal lesions by means of advanced diffusion MRI.** *Neuroradiology* 2019;61:1033–45 [CrossRef Medline](#)
8. Cramer SC, Nelles G, Benson RR, et al. **Functional MRI study of subjects recovered from hemiparetic stroke.** *Stroke* 1997;28:2518–27 [CrossRef Medline](#)
9. Hatem SM, Saussez G, Della Faille M, et al. **Rehabilitation of motor function after stroke: a multiple systematic review focused on techniques to stimulate upper extremity recovery.** *Front Hum Neurosci* 2016;10:442 [CrossRef Medline](#)
10. Liang D, Bhatta S, Gerzanich V, et al. **Cytotoxic edema: mechanisms of pathological cell swelling.** *Neurosurg Focus* 2007;22:E2 [CrossRef Medline](#)
11. Goyal M, Ospel JM, Menon B, et al. **Challenging the ischemic core concept in acute ischemic stroke imaging.** *Stroke* 2020;51:3147–55 [CrossRef Medline](#)

12. Hori N, Carpenter DO. **Functional and morphological changes induced by transient in vivo ischemia.** *Exp Neurol* 1994;129:279–89 [CrossRef Medline](#)
13. Baron CA, Kate M, Gioia L, et al. **Reduction of diffusion-weighted imaging contrast of acute ischemic stroke at short diffusion times.** *Stroke* 2015;46:2136–41 [CrossRef Medline](#)
14. Zuo M, Guo H, Wan T, et al. **Wallerian degeneration in experimental focal cortical ischemia.** *Brain Res Bull* 2019;149:194–202 [CrossRef Medline](#)
15. Jones TA, Schallert T. **Overgrowth and pruning of dendrites in adult rats recovering from neocortical damage.** *Brain Res* 1992;581:156–60 [CrossRef Medline](#)
16. Jones TA, Adkins DL. **Motor system reorganization after stroke: stimulating and training toward perfection.** *Physiology (Bethesda)* 2015;30:358–70 [CrossRef Medline](#)
17. Alexander DC, Dyrby TB, Nilsson M, et al. **Imaging brain microstructure with diffusion MRI: practicality and applications.** *NMR Biomed* 2019;32:e3841 [CrossRef Medline](#)
18. Kiselev VG. **Fundamentals of diffusion MRI physics.** *NMR Biomed* 2017;30 [CrossRef Medline](#)
19. Hagmann P, Jonasson L, Maeder P, et al. **Understanding diffusion MR imaging techniques: from scalar diffusion-weighted imaging to diffusion tensor imaging and beyond.** *Radiographics* 2006;26 (Suppl 1):S205–23 [Medline](#)
20. Novikov DS, Kiselev VG, Jespersen SN. **On modeling.** *Magn Reson Med* 2018;79:3172–93 [CrossRef Medline](#)
21. Tuch DS. **Q-ball imaging.** *Magn Reson Med* 2004;52:1358–72 [CrossRef Medline](#)
22. Concha L. **A macroscopic view of microstructure: using diffusion-weighted images to infer damage, repair, and plasticity of white matter.** *Neuroscience* 2014;276:14–28 [CrossRef Medline](#)
23. Fukutomi H, Glasser MF, Zhang H, et al. **Neurite imaging reveals microstructural variations in human cerebral cortical gray matter.** *Neuroimage* 2018;182:488–99 [CrossRef Medline](#)
24. Palombo M, Ianus A, Guerrieri M, et al. **SANDI: A compartment-based model for non-invasive apparent soma and neurite imaging by diffusion MRI.** *Neuroimage* 2020;215:116835 [CrossRef Medline](#)
25. Boscolo Galazzo I, Brusini L, Obertino S, et al. **On the viability of diffusion MRI-based microstructural biomarkers in ischemic stroke.** *Front Neurosci* 2018;12:92 [CrossRef Medline](#)
26. Schaefer PW, Grant PE, Gonzalez RG. **Diffusion-weighted MR imaging of the brain.** *Radiology* 2000;217:331–45 [CrossRef Medline](#)
27. Duong TQ, Ackerman JJ, Ying HS, et al. **Evaluation of extra- and intracellular apparent diffusion in normal and globally ischemic rat brain via 19F NMR.** *Magn Reson Med* 1998;40:1–13 [CrossRef Medline](#)
28. Jelescu IO, Veraart J, Fieremans E, et al. **Degeneracy in model parameter estimation for multi-compartmental diffusion in neuronal tissue.** *NMR Biomed* 2016;29:33–47 [CrossRef Medline](#)
29. Dhital B, Reiser M, Kellner E, et al. **Intra-axonal diffusivity in brain white matter.** *Neuroimage* 2019;189:543–50 [CrossRef Medline](#)
30. Lampinen B, Szczepankiewicz F, Martensson J, et al. **Towards unconstrained compartment modeling in white matter using diffusion-relaxation MRI with tensor-valued diffusion encoding.** *Magn Reson Med* 2020;84:1605–23 [CrossRef Medline](#)
31. Budde MD, Frank JA. **Neurite beading is sufficient to decrease the apparent diffusion coefficient after ischemic stroke.** *Proc Natl Acad Sci U S A* 2010;107:14472–77 [CrossRef Medline](#)
32. Datar A, Ameeramja J, Bhat A, et al. **The roles of microtubules and membrane tension in axonal beading, retraction, and atrophy.** *Biophys J* 2019;117:880–91 [CrossRef Medline](#)
33. Brugieres P, Thomas P, Maraval A, et al. **Water diffusion compartmentation at high b values in ischemic human brain.** *AJNR Am J Neuroradiol* 2004;25:692–68 [Medline](#)
34. Nilsson M, van Westen D, Stahlberg F, et al. **The role of tissue microstructure and water exchange in biophysical modelling of diffusion in white matter.** *MAGMA* 2013;26:345–70 [CrossRef Medline](#)
35. Lampinen B, Latt J, Wasselius J, et al. **Time dependence in diffusion MRI predicts tissue outcome in ischemic stroke patients.** *Magn Reson Med* 2021;86:754–64 [CrossRef Medline](#)
36. Kruetzelmann A, Kohrmann M, Sobesky J, et al. **Pretreatment diffusion-weighted imaging lesion volume predicts favorable outcome after intravenous thrombolysis with tissue-type plasminogen activator in acute ischemic stroke.** *Stroke* 2011;42:1251–54 [CrossRef Medline](#)
37. Campbell BC, Tu HT, Christensen S, et al. **Assessing response to stroke thrombolysis: validation of 24-hour multimodal magnetic resonance imaging.** *Arch Neurol* 2011;69:45–50 [CrossRef Medline](#)
38. Kim B, Winstein C. **Can neurological biomarkers of brain impairment be used to predict poststroke motor recovery? A systematic review.** *Neurorehabil Neural Repair* 2017;31:3–24 [CrossRef Medline](#)
39. Kwah LK, Herbert RD. **Prediction of walking and arm recovery after stroke: a critical review.** *Brain Sci* 2016;6:53 [CrossRef Medline](#)
40. Hemmen TM, Ernstrom K, Raman R. **Two-hour improvement of patients in the National Institute of Neurological Disorders and Stroke trials and prediction of final outcome.** *Stroke* 2011;42:3163–67 [CrossRef Medline](#)
41. Prabhakaran S, Zarahn E, Riley C, et al. **Inter-individual variability in the capacity for motor recovery after ischemic stroke.** *Neurorehabil Neural Repair* 2008;22:64–71 [CrossRef Medline](#)
42. Krakauer JW, Marshall RS. **The proportional recovery rule for stroke revisited.** *Ann Neurol* 2015;78:845–47 [CrossRef Medline](#)
43. Winters C, van Wegen EE, Daffertshofer A, et al. **Generalizability of the proportional recovery model for the upper extremity after an ischemic stroke.** *Neurorehabil Neural Repair* 2015;29:614–22 [CrossRef Medline](#)
44. Stinear CM, Byblow WD, Ackerley SJ, et al. **Proportional motor recovery after stroke: implications for trial design.** *Stroke* 2017;48:795–98 [CrossRef Medline](#)
45. Fugl-Meyer AR, Jaasko L, Leyman I, et al. **The post-stroke hemiplegic patient, I; a method for evaluation of physical performance.** *Scand J Rehabil Med* 1975;7:13–31 [Medline](#)
46. Hawe RL, Scott SH, Dukelow SP. **Taking proportional out of stroke recovery.** *Stroke* 2018 Dec 7. [Epub ahead of print] [CrossRef Medline](#)
47. Hope TM, Friston K, Price CJ, et al. **Recovery after stroke: not so proportional after all?** *Brain* 2019;142:15–22 [CrossRef Medline](#)
48. Farr TD, Wegener S. **Use of magnetic resonance imaging to predict outcome after stroke: a review of experimental and clinical evidence.** *J Cereb Blood Flow Metab* 2010;30:703–17 [CrossRef Medline](#)
49. Sun C, Liu X, Bao C, et al. **Advanced non-invasive MRI of neuroplasticity in ischemic stroke: techniques and applications.** *Life Sci* 2020;261:118365 [CrossRef Medline](#)
50. Albers GW, Thijs VN, Wechsler L, et al; DEFUSE Investigators. **Magnetic resonance imaging profiles predict clinical response to early reperfusion: the diffusion and perfusion imaging evaluation for understanding stroke evolution (DEFUSE) study.** *Ann Neurol* 2006;60:508–17 [CrossRef Medline](#)
51. Qiu M, Darling WG, Morecraft RJ, et al. **White matter integrity is a stronger predictor of motor function than BOLD response in patients with stroke.** *Neurorehabil Neural Repair* 2011;25:275–84 [CrossRef Medline](#)
52. Carter AR, Shulman GL, Corbetta M. **Why use a connectivity-based approach to study stroke and recovery of function?** *NeuroImage* 2012;62:2271–80 [CrossRef Medline](#)
53. Zhu LL, Lindenberg R, Alexander MP, et al. **Lesion load of the corticospinal tract predicts motor impairment in chronic stroke.** *Stroke* 2010;41:910–15 [CrossRef Medline](#)
54. Kumar MA, Vangala H, Tong DC, et al. **MRI guides diagnostic approach for ischaemic stroke.** *J Neurol Neurosurg Psychiatry* 2011;83:1201–05 [CrossRef Medline](#)
55. Song J, Nair VA, Young BM, et al. **DTI measures track and predict motor function outcomes in stroke rehabilitation utilizing BCI technology.** *Front Hum Neurosci* 2015;9:195 [CrossRef Medline](#)

56. Puig J, Pedraza S, Blasco G, et al. Wallerian degeneration in the corticospinal tract evaluated by diffusion tensor imaging correlates with motor deficit 30 days after middle cerebral artery ischemic stroke. *AJNR Am J Neuroradiol* 2010;31:1324–30 [CrossRef Medline](#)
57. Groisser BN, Copen WA, Singhal AB, et al. Corticospinal tract diffusion abnormalities early after stroke predict motor outcome. *Neurorehabil Neural Repair* 2014;28:751–60 [CrossRef Medline](#)
58. Jang SH, Lee J, Lee MY, et al. Prediction of motor outcome using remaining corticospinal tract in patients with pontine infarct: diffusion tensor imaging study. *Somatosens Mot Res* 2016;33:99–103 [CrossRef Medline](#)
59. Pannek K, Chalk JB, Finnigan S, et al. Dynamic corticospinal white matter connectivity changes during stroke recovery: a diffusion tensor probabilistic tractography study. *J Magn Reson Imaging* 2009;29:529–36 [CrossRef Medline](#)
60. Kim KH, Kim YH, Kim MS, et al. Prediction of motor recovery using diffusion tensor tractography in supratentorial stroke patients with severe motor involvement. *Ann Rehabil Med* 2015;39:570–76 [CrossRef Medline](#)
61. Frank LR. Anisotropy in high angular resolution diffusion-weighted MRI. *Magn Reson Med* 2001;45:935–39 [CrossRef Medline](#)
62. Tuch DS, Reese TG, Wiegell MR, et al. High angular resolution diffusion imaging reveals intravoxel white matter fiber heterogeneity. *Magn Reson Med* 2002;48:577–82 [CrossRef Medline](#)
63. Wedeen VJ, Wang RP, Schmahmann JD, et al. Spectrum magnetic resonance imaging (DSI) tractography of crossing fibers. *Neuroimage* 2008;41:1267–77 [CrossRef Medline](#)
64. Van AT, Granziera C, Bammer R. An introduction to model-independent diffusion magnetic resonance imaging. *Top Magn Reson Imaging* 2010;21:339–54 [CrossRef Medline](#)
65. Jones DK, Knosche TR, Turner R. White matter integrity, fiber count, and other fallacies: The do's and don'ts of diffusion MRI. *Neuroimage* 2013;73:239–54 [CrossRef Medline](#)
66. Lakhani DA, Schilling KG, Xu J, et al. Advanced multicompartiment diffusion MRI models and their application in multiple sclerosis. *AJNR Am J Neuroradiol* 2020;41:751–57 [CrossRef Medline](#)
67. Jensen JH, Helpern JA, Ramani A, et al. Diffusional kurtosis imaging: the quantification of non-Gaussian water diffusion by means of magnetic resonance imaging. *Magn Reson Med* 2005;53:1432–40 [CrossRef Medline](#)
68. Lu H, Jensen JH, Ramani A, et al. Three-dimensional characterization of non-Gaussian water diffusion in humans using diffusion kurtosis imaging. *NMR Biomed* 2006;19:236–47 [CrossRef Medline](#)
69. Cheung JS, Wang E, Lo EH, et al. Stratification of heterogeneous diffusion MRI ischemic lesion with kurtosis imaging: evaluation of mean diffusion and kurtosis MRI mismatch in an animal model of transient focal ischemia. *Stroke* 2012;43:2252–54 [CrossRef Medline](#)
70. Hui ES, Du F, Huang S, et al. Spatiotemporal dynamics of diffusional kurtosis, mean diffusivity and perfusion changes in experimental stroke. *Brain Res* 2012;1451:100–09 [CrossRef Medline](#)
71. Sun PZ, Wang Y, Mandeville E, et al. Validation of fast diffusion kurtosis MRI for imaging acute ischemia in a rodent model of stroke. *NMR Biomed* 2014;27:1413–18 [CrossRef Medline](#)
72. Umesh Rudrapatna S, Wieloch T, Beirup K, et al. Can diffusion kurtosis imaging improve the sensitivity and specificity of detecting microstructural alterations in brain tissue chronically after experimental stroke? Comparisons with diffusion tensor imaging and histology. *Neuroimage* 2014;97:363–73 [CrossRef Medline](#)
73. Weber RA, Hui ES, Jensen JH, et al. Diffusional kurtosis and diffusion tensor imaging reveal different time-sensitive stroke-induced microstructural changes. *Stroke* 2015;46:545–50 [CrossRef Medline](#)
74. Wu Y, Kim J, Chan ST, et al. Comparison of image sensitivity between conventional tensor-based and fast diffusion kurtosis imaging protocols in a rodent model of acute ischemic stroke. *NMR Biomed* 2016;29:625–30 [CrossRef Medline](#)
75. Zhang S, Yao Y, Shi J, et al. The temporal evolution of diffusional kurtosis imaging in an experimental middle cerebral artery occlusion (MCAO) model. *Magn Reson Imaging* 2016;34:889–95 [CrossRef Medline](#)
76. Wang E, Wu Y, Cheung JS, et al. pH imaging reveals worsened tissue acidification in diffusion kurtosis lesion than the kurtosis/diffusion lesion mismatch in an animal model of acute stroke. *J Cereb Blood Flow Metab* 2017;37:3325–33 [CrossRef Medline](#)
77. Lu D, Jiang Y, Ji Y, et al. JOURNAL CLUB: evaluation of diffusion kurtosis imaging of stroke lesion with hemodynamic and metabolic MRI in a rodent model of acute stroke. *AJR Am J Roentgenol* 2018;210:720–27 [CrossRef Medline](#)
78. Bay V, Kjolby BF, Iversen NK, et al. Stroke infarct volume estimation in fixed tissue: Comparison of diffusion kurtosis imaging to diffusion weighted imaging and histology in a rodent MCAO model. *PLoS One* 2018;13:e0196161 [CrossRef Medline](#)
79. Cheung J, Doerr M, Hu R, et al. Refined ischemic penumbra imaging with tissue pH and diffusion kurtosis magnetic resonance imaging. *Transl Stroke Res* 2021;12:742–53 [CrossRef Medline](#)
80. Puig J, Pedraza S, Blasco G, et al. Acute damage to the posterior limb of the internal capsule on diffusion tensor tractography as an early imaging predictor of motor outcome after stroke. *AJNR Am J Neuroradiol* 2011;32:857–63 [CrossRef Medline](#)
81. Hansen B, Jespersen SN. Recent developments in fast kurtosis imaging. *Frontiers in Physics* 2017;5 [CrossRef](#)
82. Spampinato MV, Chan C, Jensen JH, et al. Diffusional kurtosis imaging and motor outcome in acute ischemic stroke. *AJNR Am J Neuroradiol* 2017;38:1328–34 [CrossRef Medline](#)
83. Li C, Lan C, Zhang X, et al. Evaluation of diffusional kurtosis imaging in sub-acute ischemic stroke: comparison with rehabilitation treatment effect. *Cell Transplant* 2019;28:1053–61 [CrossRef Medline](#)
84. Yu X, Jiaerken Y, Wang S, et al. Changes in the corticospinal tract beyond the ischemic lesion following acute hemispheric stroke: a diffusion kurtosis imaging study. *J Magn Reson Imaging* 2020;52:512–19 [CrossRef Medline](#)
85. Chung S, Fieremans E, Wang X, et al. White matter tract integrity: an indicator of axonal pathology after mild traumatic brain injury. *J Neurotrauma* 2018;35:1015–20 [CrossRef Medline](#)
86. Wedeen VJ, Hagmann P, Tseng WY, et al. Mapping complex tissue architecture with diffusion spectrum magnetic resonance imaging. *Magn Reson Med* 2005;54:1377–86 [CrossRef Medline](#)
87. Jiang Q, Zhang ZG, Chopp M. MRI evaluation of white matter recovery after brain injury. *Stroke* 2010;41:S112–13 [CrossRef Medline](#)
88. Tang PF, Ko YH, Luo ZA, et al. Tract-specific and region of interest analysis of corticospinal tract integrity in subcortical ischemic stroke: reliability and correlation with motor function of affected lower extremity. *AJNR Am J Neuroradiol* 2010;31:1023–30 [CrossRef Medline](#)
89. Granziera C, Daducci A, Gigandet X, et al. Diffusion spectrum imaging after stroke shows structural changes in the contra-lateral motor network correlating with functional recovery. In: *Proceedings of the International Society for Magnetic Resonance in Medicine Conference*, Montreal, Quebec, Canada. May 7–13, 2011
90. Ozarslan E, Koay CG, Shepherd TM, et al. Mean apparent propagator (MAP) MRI: a novel diffusion imaging method for mapping tissue microstructure. *Neuroimage* 2013;78:16–32 [CrossRef Medline](#)
91. Brusini L, Obertino S, Galazzo IB, et al. Ensemble average propagator-based detection of microstructural alterations after stroke. *Int J Comput Assist Radiology Surg* 2016;11:1585–97 [CrossRef Medline](#)
92. Zhang H, Schneider T, Wheeler-Kingshott CA, et al. NODDI: practical in vivo neurite orientation dispersion and density imaging of the human brain. *Neuroimage* 2012;61:1000–16 [CrossRef Medline](#)
93. Anderova M, Vorisek I, Pivonkova H, et al. Cell death/proliferation and alterations in glial morphology contribute to changes in diffusivity in the rat hippocampus after hypoxia-ischemia. *J Cereb Blood Flow Metab* 2011;31:894–907 [CrossRef Medline](#)

94. Bagdasarian FA, Yuan X, Athey J, et al. **NODDI highlights recovery mechanisms in white and gray matter in ischemic stroke following human stem cell treatment.** *Magn Reson Med* 2021;86:3211–23 [CrossRef Medline](#)
95. Adluru G, Gur Y, Anderson J, et al. **Assessment of white matter microstructure in stroke patients using NODDI.** *Annu Int Conf IEEE Eng Med Biol Soc* 2014;2014:742–45 [CrossRef Medline](#)
96. Hodgson K, Adluru G, Richards LG, et al. **Predicting motor outcomes in stroke patients using diffusion spectrum MRI microstructural measures.** *Front Neurol* 2019;10:72 [CrossRef Medline](#)
97. Wang Z, Zhang S, Liu C, et al. **A study of neurite orientation dispersion and density imaging in ischemic stroke.** *Magn Reson Imaging* 2019;57:28–33 [CrossRef Medline](#)
98. Latt J, Nilsson M, van Westen D, et al. **Diffusion-weighted MRI measurements on stroke patients reveal water-exchange mechanisms in sub-acute ischaemic lesions.** *NMR Biomed* 2009;22:619–28 [CrossRef Medline](#)
99. Barrio-Arranz G, de Luis GR, Tristan-Vega A, et al. **Impact of MR acquisition parameters on DTI scalar indexes: a tractography based approach.** *PLoS One* 2015;10:e0137905 [CrossRef Medline](#)
100. Parvathaneni P, Nath V, Blaber JA, et al. **Empirical reproducibility, sensitivity, and optimization of acquisition protocol, for neurite orientation dispersion and density imaging using AMICO.** *Magn Reson Imaging* 2018;50:96–109 [CrossRef Medline](#)
101. Bergamino M, Keeling EG, Walsh RR, et al. **Systematic assessment of the impact of DTI methodology on fractional anisotropy measures in Alzheimer's disease.** *Tomography* 2021;7:20–38 [CrossRef Medline](#)
102. Daducci A, Canales-Rodriguez EJ, Zhang H, et al. **Accelerated Microstructure Imaging via Convex Optimization (AMICO) from diffusion MRI data.** *Neuroimage* 2015;105:32–44 [CrossRef Medline](#)
103. HashemizadehKolowri K, Chen RR, Adluru G, et al. **Simultaneous multi-slice image reconstruction using regularized image domain split slice-GRAPPA for diffusion MRI.** *Med Image Anal* 2021;70:102000 [CrossRef Medline](#)
104. Ye C, Li Y, Zeng X. **An improved deep network for tissue microstructure estimation with uncertainty quantification.** *Med Image Anal* 2020;61:101650 [CrossRef Medline](#)
105. Bundy DT, Souders L, Baranyai K, et al. **Contralesional brain-computer interface control of a powered exoskeleton for motor recovery in chronic stroke survivors.** *Stroke* 2017;48:1908–15 [CrossRef Medline](#)